

Reconstruction of the chaotic set from classical cross section data

This article has been downloaded from IOPscience. Please scroll down to see the full text article.

2005 J. Phys. A: Math. Gen. 38 567

(<http://iopscience.iop.org/0305-4470/38/3/004>)

View [the table of contents for this issue](#), or go to the [journal homepage](#) for more

Download details:

IP Address: 171.66.16.92

The article was downloaded on 03/06/2010 at 03:51

Please note that [terms and conditions apply](#).

Reconstruction of the chaotic set from classical cross section data

C Jung¹, G Orellana-Rivadeneyra² and G A Luna-Acosta^{3,4}

¹ Centro de Ciencias Físicas, UNAM, Apartado Postal 48-3, Cuernavaca, México

² Instituto de Física, BUAP, Apartado Postal J-48, 72570 Puebla, México

³ Fachbereich Physik der Philipps Universität Marburg, Renthof 5, D-35032, Germany

E-mail: gluna@sirio.ifuap.buap.mx

Received 17 July 2004, in final form 24 October 2004

Published 23 December 2004

Online at stacks.iop.org/JPhysA/38/567

Abstract

We study a paradigm of a chaotic scattering system with one open and one closed degree of freedom. We show how the development scenario of the chaotic invariant set is reflected in the changes of the rainbow singularities in the classical cross section. This allows us to reconstruct the actual development stage of the chaotic set from the knowledge of the cross section. We do this by following the rainbow structure of the cross section along a curve in parameter space which connects the case we are interested in with a known case, for example, the case of a complete horseshoe. We conclude with a discussion about the generality of our procedure and of its application to various systems.

PACS numbers: 05.45.–a, 72.10.Fr

1. Introduction

When we hear the expression ‘inverse scattering problem’ then traditionally we think of the reconstruction of a scattering potential or of a Hamiltonian function from scattering data [1–3]. While for rotationally symmetric and monotonic potentials this problem is solved in closed form, for general interactions this inversion contains ambiguities, and small changes in the initial data can lead to qualitatively different potentials. Assuming we have reconstructed a reasonable potential, we then would have to extract its dynamical properties in order to reach the usual final goal of having a qualitative understanding of the system under study. Thus, it would be a great advantage if we could determine the important qualitative properties of the dynamics directly from the scattering data without having to reconstruct the potential, a deviation that may lead to further possibilities for errors.

⁴ On sabbatical leave from Instituto de Física, BUAP.

If the underlying dynamics is chaotic then the properties in which we are interested are the topological structure of the horseshoe construction in a corresponding Poincaré map and the scaling factors of the system which determine the measures of chaos (for an overview of the whole area of chaotic scattering see the feature issue of the journal *CHAOS* [4]). Several recent attempts [5–8] to reconstruct the topology of the chaotic invariant set started from the analysis of the fractal structure of the singularities in scattering functions, since it coincides with the fractal structure of the horseshoe. Once we have the hierarchical structure of this fractal, we can measure its scaling factors and apply the thermodynamical formalism to extract all measures of chaos [9]. The disadvantage of doing all this work is that it starts from scattering functions whose measurements require the simultaneous preparation of canonically conjugate variables. In classical dynamics this is possible, at least conceptionally. However, this is usually not done in real scattering experiments and, moreover, these methods thereby never allow any generalization to quantum dynamics, where the simultaneous preparation of conjugate variables is forbidden in principle.

Therefore, in the present paper we discuss the possibility to extract the desired information from cross section data only. Cross sections are the quantities which are measured directly in most real scattering experiments. Furthermore, cross sections are quantities which have in classical dynamics and in quantum dynamics the same meaning and same definition. Therefore, any procedure based only on cross sections has a good chance to be generalized to quantum dynamics. In this spirit, the purpose for the present paper is to show how we can extract information on the topology of the chaotic set and on important scaling factors, assuming that the classical cross section data for an open two degree of freedom system are given. We use scattering functions only as auxiliary quantities to explain and motivate the ideas but we do not need them in the end to do the reconstruction.

Our work here is motivated by the study of the transport of particles in two-dimensional configuration space when their motion is channelled (i.e., bounded in the transverse direction by some potential) and in the presence of some localized scatterer, e.g., an impurity or a defect. Therefore, we restrict the considerations to systems with one open and one closed degree of freedom and use, as example of demonstration, a model of a channel system that will be specified shortly. The physical importance and interpretation of the model will be given in another place [10]; here, we concentrate on the inverse scattering problem only. Systems of the same qualitative structure can also be realized by co-linear scattering of a particle from a bound state of two particles, where vibrational excitation of the bound system takes place. In addition, the same basic structure is found in externally periodically driven scattering systems with a one-dimensional position space. In the last section, we discuss the generality of the procedure developed here.

2. The system and its coordinates

For the open degree of freedom we use the conjugate position and momentum coordinates X and \mathcal{P}_x , and for the closed one we may use either the position and momentum coordinates Y and \mathcal{P}_y or their corresponding action and angle coordinates \mathcal{I} and ϕ . The asymptotic region is the limit of large absolute values of X . In the asymptotic region the motion is free motion along the channel and an independent harmonic vibrational motion perpendicular to it. Accordingly, the asymptotic Hamiltonian \mathcal{H}_0 is

$$\mathcal{H}_0 = \frac{\mathcal{P}_x^2}{2m} + \frac{\mathcal{P}_y^2}{2m} + \frac{m\omega^2 Y^2}{2} = \frac{\mathcal{P}_x^2}{2m} + \omega\mathcal{I}, \quad (1)$$

The classical motion of ballistic electrons in a uniform 2D electron wave guide, a 2D electron gas confined transversely by a gate potential, is precisely governed by the Hamiltonian \mathcal{H}_0 .

The form of the confining potential is typically parabolic [11], as we have assumed here. Now we include in the channel an obstacle centred at the origin of the position space, creating an additional potential \mathcal{V} . Specifically, we shall consider the case of an obstacle represented by an attractive, screened regularized Coulomb potential,

$$\mathcal{V}(X, Y) = -c_0 \frac{\exp[-\Delta^{-1}(X^2 + Y^2 + \delta^2)^{1/2}]}{(X^2 + Y^2 + \delta^2)^{1/2}}. \quad (2)$$

Here, c_0 is the strength of the electrostatic interaction between an electron in the channel and the impurity Δ is the Debye length, which is the effective range of the impurity and δ is the smallest distance of approach to the impurity. There are several theoretical works that study electron transport in wave guides in the presence of few isolated impurities, see [12]. Their description is purely quantum mechanical, and for simplicity the lateral confinement is modelled by hard straight walls, and the impurities by delta functions or Gaussian functions in one degree of freedom. We are considering here the more realistic case of parabolic confinement and screened coulomb impurities. The quantum version of this system is currently under investigation.

By writing the energies in units of $m\omega^2\Delta^2$, distances in units of Δ , momenta in units of $m\omega\Delta$ and transforming to action angle variables ($I = \frac{p_x^2}{2} + \frac{y^2}{2}$, $\phi = \tan^{-1}(\frac{y}{p_x})$) of the harmonic oscillator, the total Hamiltonian is given by

$$H = H_0 + V(x, I, \phi), \quad (3)$$

where

$$H_0 = \frac{p_x^2}{2} + I \quad (4)$$

and

$$V(x, I, \phi) = -C \frac{\exp[-(x^2 + 2I \sin^2 \phi + (\delta/\Delta)^2)^{1/2}]}{(x^2 + 2I \sin^2 \phi + (\delta/\Delta)^2)^{1/2}}. \quad (5)$$

The adimensional coupling constant $C = \frac{c_0}{m\omega\Delta^3}$. In this work, we will use for concreteness $\delta/\Delta = 1$ (a deep impurity), without loss of generality of the method.

Convenient labels for asymptotic trajectories are the following quantities which are conserved under the asymptotic motion: the total energy E , the action I and the reduced phase $\tilde{\phi} = \phi - \omega m X / |P_x| = \phi - x / |p_x|$.

The maximal value I_{\max} of the action in the asymptotic region for fixed value E of the total energy is given by $I_{\max} = E$, i.e., when all the energy is in the vibrational degree of freedom. For a given total energy, we can only prepare asymptotic initial conditions with $I < I_{\max}$ and, as a result of a scattering event, only values fulfilling this inequality can come out.

3. Development scenario of the homoclinic/heteroclinic tangle

The chaotic invariant set can be represented by a horseshoe construction in an appropriate Poincare section. The system has two different discrete symmetries of order 2: the reflection $x \rightarrow -x$ and the reflection $y \rightarrow -y$. As the surface of section we choose the plane $y = 0$ which has the following advantages: first, almost all trajectories cross this plane an infinite number of times and they do it with a finite return time. The only exceptions are the trajectories running exactly along the line $y = 0$, i.e., trajectories with action $I = 0$. Second, this plane is invariant under the symmetry $y \rightarrow -y$ of the Hamiltonian. Therefore, we can make a symmetry reduction of the Poincare map by simply taking both orientations of intersection with this plane. The other symmetry ($x \rightarrow -x$) will show up in the Poincare plots.

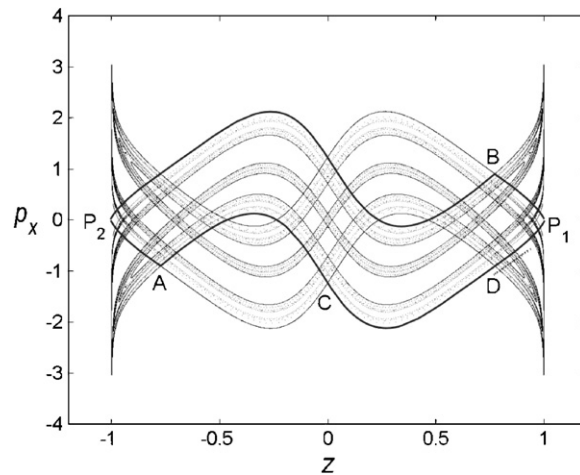


Figure 1. Horseshoe well within the parameter region of the complete case ($\beta = 1$). $z = \tanh(x/A)$. Parameter values $E = 17$, $C = 36$. The fundamental rectangle R is bounded by thick lines.

In the plots of Poincaré sections, we use the horizontal coordinate $z = \tanh(x/A)$ to transform the infinite x -axis into the finite interval $z \in [-1, 1]$, and in particular to bring the outer fixed points at infinity into the plots. For the vertical coordinate, we use p_x .

There is a periodic trajectory oscillating on the line $x = 0$. It leads to a fixed point P_0 of the map at $z = 0$, $p_x = 0$. The stability and the eigenvalues of this fixed point depend on the parameter values. The map does not have further fixed points at finite values of x ; however, the points P_1 at $x = \infty$ ($z = 1$), $p_x = 0$ and P_2 at $x = -\infty$ ($z = -1$), $p_x = 0$ act as the outer fixed points of the map. These points represent the oscillation of the particle in the y -direction at a fixed value of x if the absolute values of x goes to very large values where the dynamics is governed by H_0 only. Since this trajectory is invariant under small shifts in x -direction, it is parabolic; the eigenvalues of the corresponding fixed point of the map are 1.

Correspondingly, the chaotic invariant set is represented in the Poincaré section by a ternary symmetric horseshoe with outer fixed points P_1 and P_2 at $x = \pm\infty$, i.e., $z = \pm 1$ and $p_x = 0$. The horseshoe construction is traced out by the invariant manifolds of the outer fixed points. The local segments of these manifolds represent trajectories whose x coordinate diverges monotonically to $\pm\infty$ while at the same time the p_x coordinate converges to zero. In figures 1 and 2, we show this horseshoe construction for two different values of the system parameters. They represent development stages $\beta = 1$ and $\beta = 8/9$, where β is the *development parameter* explained in [5], used to characterize the topology of the homoclinic/heteroclinic tangle of the two outer fixed points. It measures how deep the first level gaps penetrate into the fundamental area of the horseshoe compared to the complete case. The parameter value $\beta = 1$ labels a complete ternary symmetric horseshoe whose symbolic dynamics is given by a complete shift in three symbol values.

The curvilinear quadrangle having as boundaries the local branches of the invariant manifolds of the outer fixed points is the fundamental rectangle R of the horseshoe construction. It covers all localized trajectories of the map. Its four corners are the outer fixed points P_1 and P_2 and the primary heteroclinic intersection points A and B marked in the figures. In the figures, R is bounded by thick lines. If we continue the invariant manifolds beyond the intersection points A and B they start to form tendrils. We then identify some segments of the manifolds. Consider, for example, the stable manifold coming from the left outer fixed

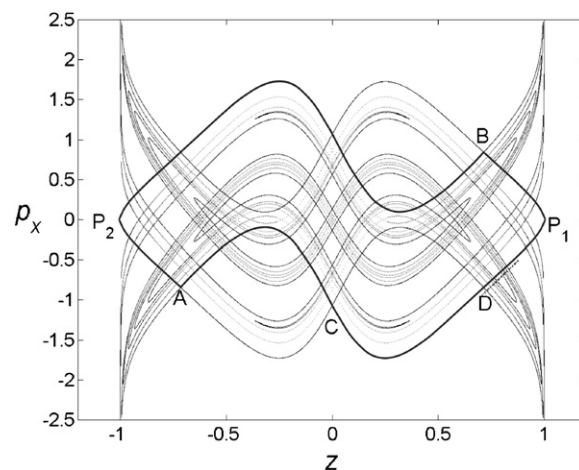


Figure 2. Horseshoe for $\beta = 8/9$ used later in section 5. $z = \tanh(x/A)$. Parameter values $E = 17$, $C = 26.3$. The fundamental rectangle R is bounded by thick lines.

point, i.e., the point P_2 . It is the line starting from P_2 and passing the points A , C and D . The segment between the points A and C forms the *stable outer tendril of level 1* coming from point P_2 . The segment between the points C and D forms the *inner stable gap of level 1* coming from the point P_2 . By symmetry, analogous segmentation is done for the other manifolds. The preimage of the outer stable tendril of level n is the outer stable tendril of level $n + 1$. The preimage of the inner stable gap of level n is the inner stable gap of level $n + 1$. Note that higher order inner gaps reach into the tendrils and form an inner fractal structure of the tendrils.

It is known that horseshoes can be hyperbolic even though they may be incomplete (see, e.g., [13]). In our system, hyperbolic incomplete cases cannot occur because, as mentioned above, the outer fixed points are parabolic with eigenvalues 1.

There exists an infinite number of values of β of the form $k/3^n$ (k any natural number not divisible by 3 and less than 3^n) whose corresponding development stages of the homoclinic/heteroclinic tangle are realized in *intervals* in the space of the physical parameters. However, there is also an infinite set of the same form $k/3^n$ which are not realized as intervals in the development stages of horseshoes. Comparing the two development stages shown in the two figures note that in figure 2 the first stable gap does not penetrate R completely; it ends in that part of the unstable gap of level 2 which lies closest to the opposite boundary of R . This situation defines the development stage $\beta = 8/9$.

In figure 3, we show in the parameter space the boundaries of some of the most important development stages. Including the infinity of less important development stages would create a devils staircase. One part of the inverse chaotic scattering problem consists in finding out from scattering data on which step of this staircase the actual case under study is located. Note that because of the problem to keep parameters sufficiently close to constant it only makes sense to investigate cases which are realized on sufficiently wide steps of the staircase. Other cases are too unstable against tiny changes of physical parameters. In section 5, we shall give an answer to this problem of reconstruction and treat as example of demonstration the case $\beta = 8/9$.

In figures 1 and 2, we included as dotted line (near the segment from P_1 to D) a line which lies close to the local branch of an unstable manifold but outside the fundamental rectangle of the horseshoe and which cuts a complete outer tendril of the stable manifolds once. Later this

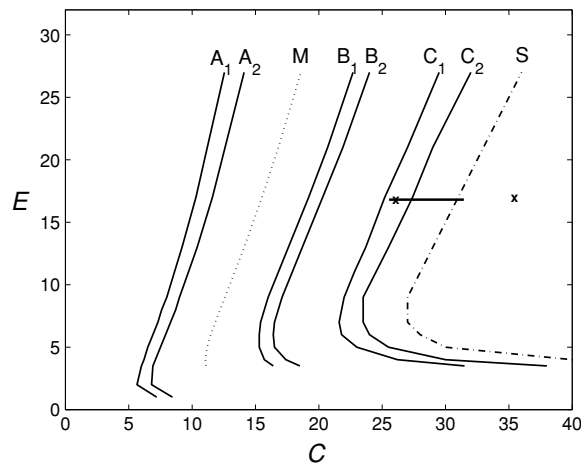


Figure 3. The dependence of the development stage β on the physical parameters C and E . The strips of the important stages $1/3$, $2/3$ and $8/9$ are shown, their boundaries are the continuous lines labelled by A_1 , A_2 , B_1 , B_2 and C_1 , C_2 , respectively. The boundary of the infinite region where the development stage 1 occurs is given by the dashed-dotted line S . The development $1/2$ is not a strip of nonzero width, it is only a line represented as the dotted curve M . The parameter values of figures 1 and 2 are marked by 'X'; the horizontal line is an interval studied in detail in sections 4–6.

type of lines will play an important role. Then we must understand some important structures along these lines. The inner gaps reach into the outer tendrils and create an internal fractal structure of gaps which are empty of other branches. Let us concentrate firstly on the complete case of figure 1. The innermost part of the dotted line intersects the gap of level 1 in the middle. Between this middle gap and the boundary of the tendrils are two different gaps of level 2 on either side. On the next level 3 there are two gaps in between each pair of adjacent gaps of lower level or between gaps of lower level and the boundary. This scheme continues to higher levels. In total we find 1 gap of level 1 and $4 \times 3^{n-2}$ gaps for the higher levels n in the case $\beta = 1$ of a complete ternary horseshoe.

In contrast, for the incomplete cases a part of these inner gaps has already disappeared. Therefore, the incomplete cases have fewer inner gaps. For example, for the case $\beta = 8/9$ shown in figure 2, the gap of level 1 in the middle has already disappeared, the four gaps of level 2 are still present without qualitative change, from the 12 gaps of level 3 one has disappeared completely and two other ones have fused together. To identify a development stage of the form $\beta = k/3^n$ uniquely it is sufficient to know the intersection pattern of the dotted line with the inner gaps of a stable tendril up to level $n + 1$. And in the following sections, we shall see how we can extract this pattern from asymptotic data.

4. Scattering functions and cross sections

The important scattering function for a system with one open and one closed degree of freedom is the final action as a function of the initial reduced phase for fixed total energy and fixed initial action. Figures 4 and 5 show these scattering functions for the parameter values belonging to the horseshoes shown in figures 1 and 2, respectively. Figure 4(a) shows the function on its complete domain. Note that because of symmetry reasons the functions are periodic with period π . Figure 4(b) shows a magnification of the part containing singularities

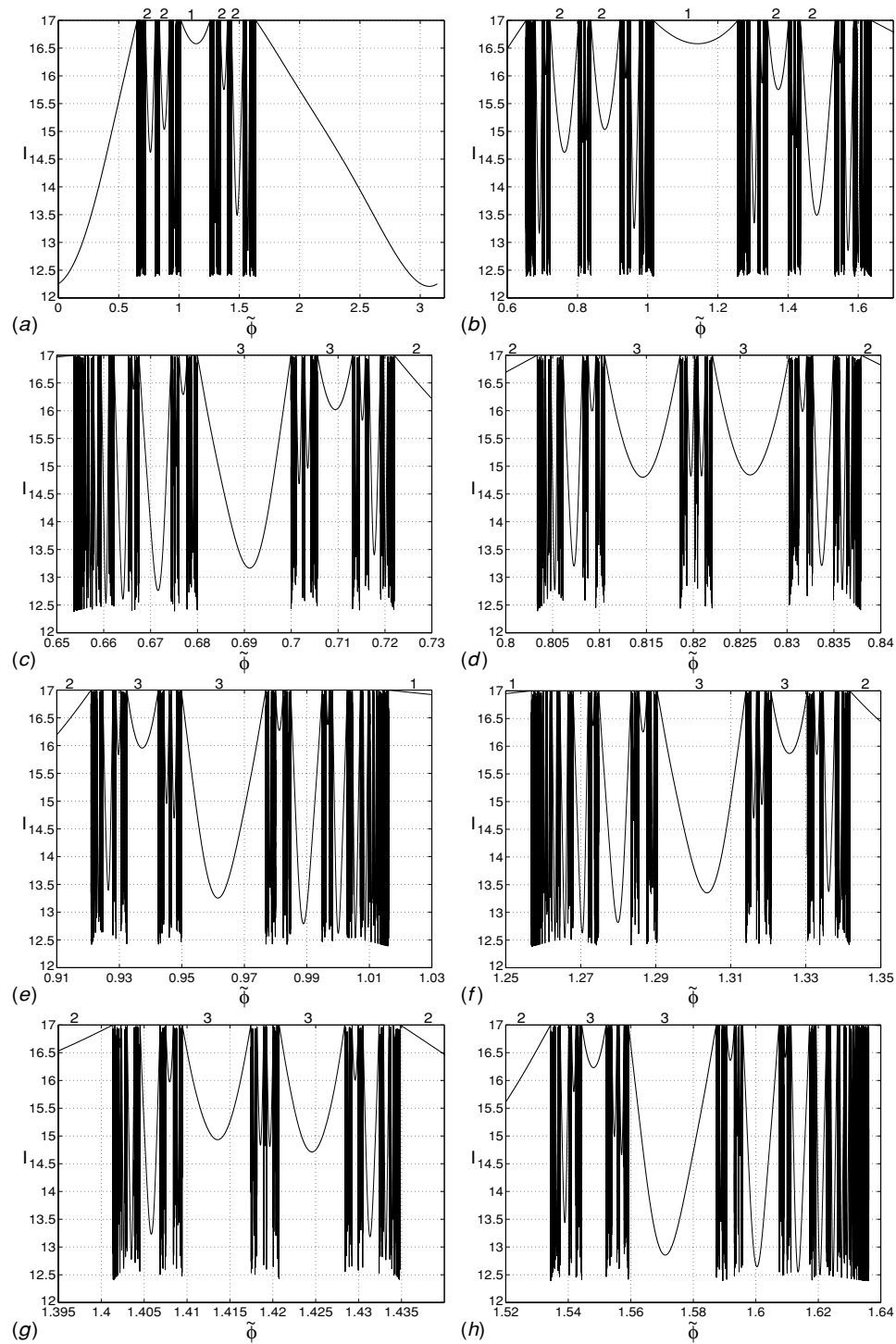


Figure 4. Scattering function and some magnifications for a complete horseshoe case. $E = 17$, $C = 36$. The intervals of continuity of hierarchical level up to 3 are labelled by the hierarchy number.

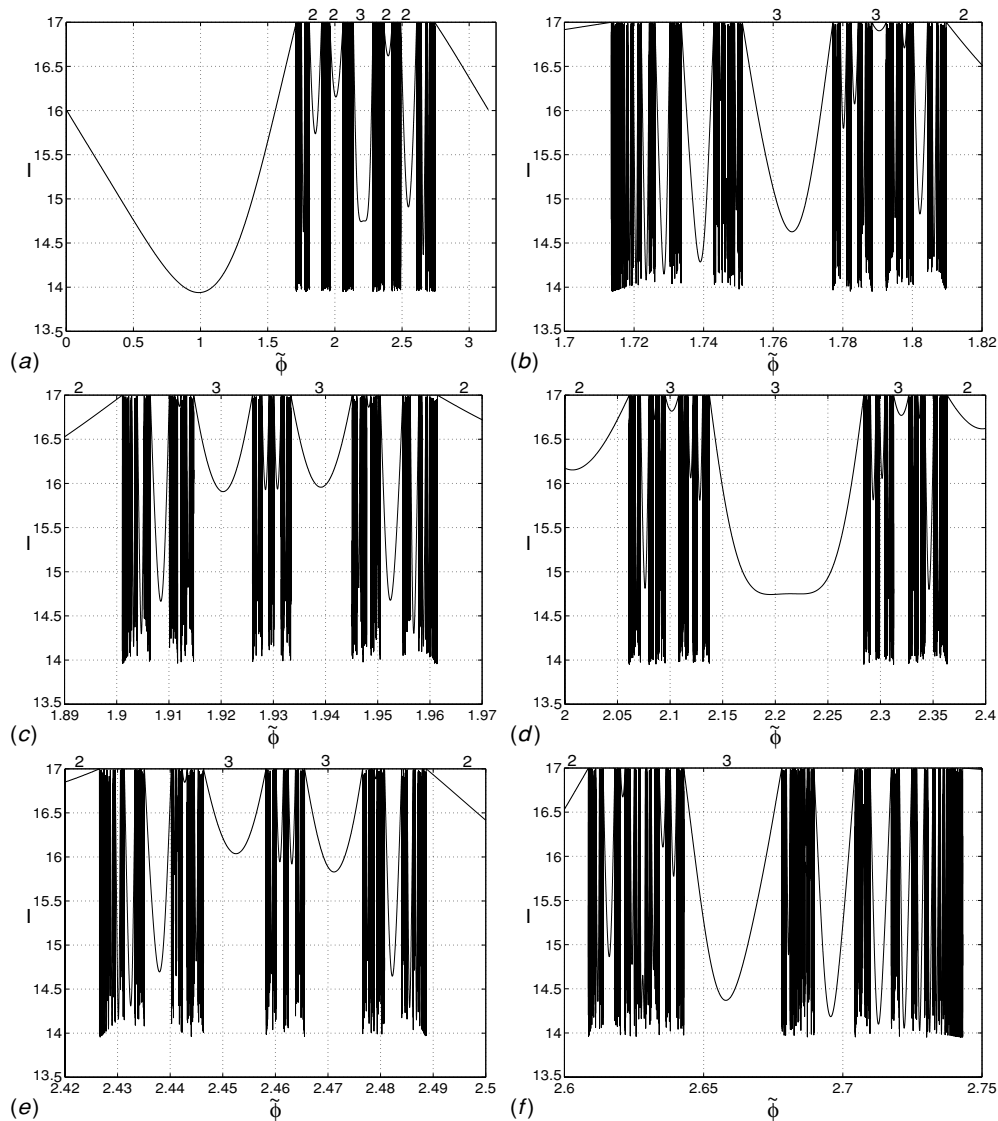


Figure 5. Scattering function and magnifications for an incomplete horseshoe case ($\beta = 8/9$). $E = 17, C = 26.3$.

and parts (c)–(h) show some further magnifications. Similarly, figure 5(a) shows the complete domain and parts (b)–(f) of figure 5 show magnifications.

As always in chaotic scattering, the scattering functions have a fractal structure of singularities and intervals of continuity in between. As explained in detail in [5] it coincides with the fractal structure of the intersections of the stable manifolds of the outer fixed points with the local segments of the unstable manifolds. The essential idea is: if we select a line of initial conditions with E and I constant, and $\tilde{\phi}$ going from 0 to 2π then some iterated image of this line runs exactly like the dotted lines in figures 1 and 2. The Poincaré map maps intersections with stable manifolds into intersections with stable manifolds. Consequently, the intersection pattern of the line of initial conditions with the stable manifolds coincides

with the intersection pattern of the dotted lines in figures 1 and 2 with the stable manifolds. And hence it is a smooth image of the intersection pattern between the stable manifold and the local branch of the unstable manifold. The gaps in the interior of the tendril correspond to the intervals of continuity of the scattering function. Therefore, we could reconstruct the topology of the horseshoe immediately if we could measure the scattering function and knew the hierarchical level of each interval of continuity (in the figures all intervals of continuity up to level 3 are labelled by their level number). Unfortunately, in the general case it is difficult to know the hierarchical structure of the fractal by the analysis of asymptotic data only and it is impossible to see the hierarchical level of any interval of continuity directly from a plot of the scattering function. Furthermore, as mentioned in the introduction, it is not the scattering functions which are usually measured in experiments, but the cross sections.

In our system, the differential cross section is the following quantity: it is the relative probability to observe a final value I_f of the action if we shoot in a beam with fixed value of the total energy E , fixed value I_i of the initial action and a constant distribution of the initial reduced angle $\tilde{\phi}_i$ in the interval $(0, 2\pi)$ (in our particular example system an interval of length π is sufficient because of symmetry). If the value of I_i is chosen in an appropriate interval, then the corresponding line of initial conditions cuts a complete stable tendril of the homoclinic/heteroclinic tangle of the outer fixed points. As mentioned above, this line is a preimage of a line running very close to the local segment of an unstable manifold of either P_1 or P_2 . Therefore, the pattern of intersections of the initial line with the stable manifolds coincides with the pattern of the homoclinic/heteroclinic intersections in the horseshoe. All end points of intervals of continuity are intersection points with the stable manifolds.

From the knowledge of the scattering function $I_f(\tilde{\phi}_i)$ the value $\sigma(I_f)$ of the cross section for a particular value of I_f can be obtained as follows (for the corresponding considerations for two open degrees of freedom see [14]). Get all values $\tilde{\phi}_{i,k}$ of the initial reduced phase which lead to the desired final value of the action. Give to each contribution the weight

$$g_k = 1/|dI(\tilde{\phi})/d\tilde{\phi}|_{\tilde{\phi}_k}. \quad (6)$$

Then the cross section is the sum of all these weights

$$\sigma(I) = \sum_k g_k. \quad (7)$$

In the following, the most prominent and important structures in the cross section are the so-called *rainbow* singularities caused by relative extremal points of the scattering function (for some general background on the rainbow effect see section 5.5 in [16]). Imagine that around a nondegenerate local minimum of the scattering function located at the value $\tilde{\phi} = \alpha$ of the initial reduced angle this function can be approximated as

$$I(\tilde{\phi}) = a + b(\tilde{\phi} - \alpha)^2 \quad (8)$$

with a and b real positive numbers, where a is the value of the action in the minimum. Then for $I < a$ there is no contribution to σ and for a value $I > a$ there are two contributions from the two trajectories starting with the initial reduced phases

$$\tilde{\phi}_{1,2} = \alpha \pm \sqrt{(I - a)/b}. \quad (9)$$

The corresponding weights are equal and have the value

$$g_{1,2} = \frac{1}{2} \frac{1}{\sqrt{b(I - a)}} \quad (10)$$

and hence the contribution to the cross section from these two trajectories is twice the value given in equation (10). We see that it leads to a singularity of one over square root type exactly

at $I = a$ and the orientation of the nonzero side of the cross section is towards higher values of I . Observe that the integral in I over this singularity is finite and, therefore, there is only a finite count rate in the detector, as it must be. Let us estimate briefly this total contribution coming from any local minimum. As figures 4 and 5 suggest, the scattering function in any interval of continuity (which is not the exceptional case of two merging intervals explained below) is close to parabolic and goes to the value I_{\max} at its endpoints. Accordingly, as a rough model let us assume a scattering function of the form given by equation (8) for a complete interval of continuity going from $\tilde{\phi}_- = \alpha - \sqrt{(I_{\max} - a)/b}$ to $\tilde{\phi}_+ = \alpha + \sqrt{(I_{\max} - a)/b}$. Note that at both end points the function goes to the value I_{\max} as it should be. Then the corresponding cross section is given by twice the expression of equation (10). The integral of this function from a to I_{\max} gives just the length of the interval, i.e., $2\sqrt{(I_{\max} - a)/b}$. This result is almost trivial since we have assumed a constant density of the incoming particles along the $\tilde{\phi}$ -axis. Accordingly, the total contribution of this interval must be just its length. However, this result is useful to estimate later the lengths of intervals of continuity from the total integrated strength of the corresponding contribution in the cross section. These lengths are exactly what we need as input for the thermodynamical formalism to get the quantitative measures of the chaos.

For a local maximum of the scattering function we can make an analogous estimation and obtain again a singularity of one over square root type at the maximal value of I . However, then the nonzero side of the peak is oriented towards lower values of I .

Note that the type of system studied here offers a great advantage over the general scattering system of 2 degrees of freedom. Namely, in each interval of continuity J_k (with possibly a single exception discussed below in all detail) the scattering function has a single quadratic minimum with value $I_{k,\min}$ and goes to its maximal value $I_{\max} = E$ (which is independent of k) monotonically on both sides of the minimum. Thus, for any value of I in the open interval $(I_{k,\min}, I_{\max})$ the interval J_k contributes two trajectories and at the value $I_{k,\min}$ it produces a generic rainbow singularity in the cross section. This happens if only one degree of freedom is open and the second degree of freedom is either closed or consists of a periodic time dependence (for an example of scattering functions and cross sections in the later case see [15]). In contrast, for systems of two open degrees of freedom the scattering function gives the final angle as function of the initial impact parameter and the differential cross section is a function of scattering angle. Then usually the scattering function has an infinite sequence of relative extremal points in each interval of continuity and accordingly each interval of continuity contributes an infinite sequence of rainbow singularities in the cross section (for a representative example and detailed explanations see [14]). This is the reason why we treat here the simpler case of scattering off an obstacle in a channel.

The above property for channels with an obstacle has the following explanation. The end points of intervals of continuity are intersections of the line of initial conditions with the stable manifold of one of the fixed points at infinity. This means that the corresponding trajectory in position space diverges to infinity but its velocity along the channel converges to zero. Then also the kinetic energy of the longitudinal motion goes to zero and the total energy E is contained in the transversal motion only. Consequently, the action I of the transverse oscillation must go to its maximal possible value $I_{\max} = E$. As soon as the initial condition leaves the interval of continuity, the trajectory does no longer make it to infinity in the segment of the trajectory where it did before; instead, it turns around and makes more loops in the interaction region before leaving. Thereby, it changes its qualitative structure. In the interior of intervals of continuity the trajectory goes to infinity with a longitudinal kinetic energy different from zero. Then only the rest of the energy is contained in the transverse oscillations and hence the transverse action is smaller than I_{\max} . A rough measure of the final longitudinal

kinetic energy is the square of the distance in the momentum direction of the initial point from the middle of the interval of continuity.

In the next section, we also treat the exceptional case which happens when two intervals of continuity fuse. Then the scattering function in the new fused interval of continuity has one local maximum in between two local minima. The two minima lead to two rainbows of the type discussed above. The maximum leads to a rainbow singularity again of the one over square root type but with different orientation. If I_1 is the value of action in the maximum located at $\tilde{\phi} = \gamma$, then the contributions of trajectories with reduced angles near γ contribute in the cross section for values of the action smaller than I_1 . This is reversed compared to the case of minima discussed above. If we change parameters then the two minima come closer and collide with the maximum and the three extremal points turn into a single minimum. Figure 6 gives a sequence of plots for this event.

First in figure 6(a) we show I versus $\tilde{\phi}$ for the case of a complete horseshoe but with different parameter values from that of figure 1. Here, we observe that the two intervals we are now interested in (they are labelled by their hierarchy number 3 and marked by arrows) are separated by singularities and intervals of various levels (the large interval in the middle is of level 1). Next we change the physical parameters in small steps to approach finally the case $\beta = 8/9$. We illustrate this by changing the coupling constant C along the horizontal line drawn in figure 3. In figure 6(b) the horseshoe is already incomplete, which is reflected in the disappearance of the interval of level 1. On the way along the curve in parameter space several intervals of higher level fuse, in figure 6(c) we see such a case. And, most important, the structures between the two intervals we are now interested in become narrower and narrower on the $\tilde{\phi}$ -axis until they finally disappear. Figure 6(d) shows the case just a little before fusion and figure 6(e) is just after the fusion. Exactly at fusion a new maximum is created and the value of the maximum is I_{\max} . With further change of parameters this value of the local maximum decreases. During this event three rainbow singularities collide and turn into a single one. At the point of collision the singularity is degenerate and is of a different type. Figure 6(f) shows exactly this stage of development. Here, the scattering function can locally be approximated as

$$I(\tilde{\phi}) = a + b(\tilde{\phi} - \alpha)^4. \quad (11)$$

For $I > a$, there are two contributing trajectories at

$$\tilde{\phi} = \alpha \pm [(I - a)/b]^{1/4} \quad (12)$$

with weights

$$g_{1,2} = 1/\{4b[(I - a)/b]^{3/4}\}. \quad (13)$$

The contribution to the cross section is twice this value. We see that exactly in the collision point the singularity changes its type into one with power $-3/4$.

Under a further change of the parameters the minimum turns into a generic minimum whose value increases (see figure 6(g)). The fused intervals shrinks until it disappears completely. Figure 6(h) shows the scattering function just before the final disappearance. In the sequence of figures 6(a)–(h) note some drift of the structures along the $\tilde{\phi}$ -axis. The reason is that the zero value of $\tilde{\phi}$ depends on the parameter values.

5. Reconstruction of the horseshoe from cross section data

So far we have established the following connections: the chaotic set is characterized by the horseshoe construction in the Poincare map. And its topology is reflected in the fractal

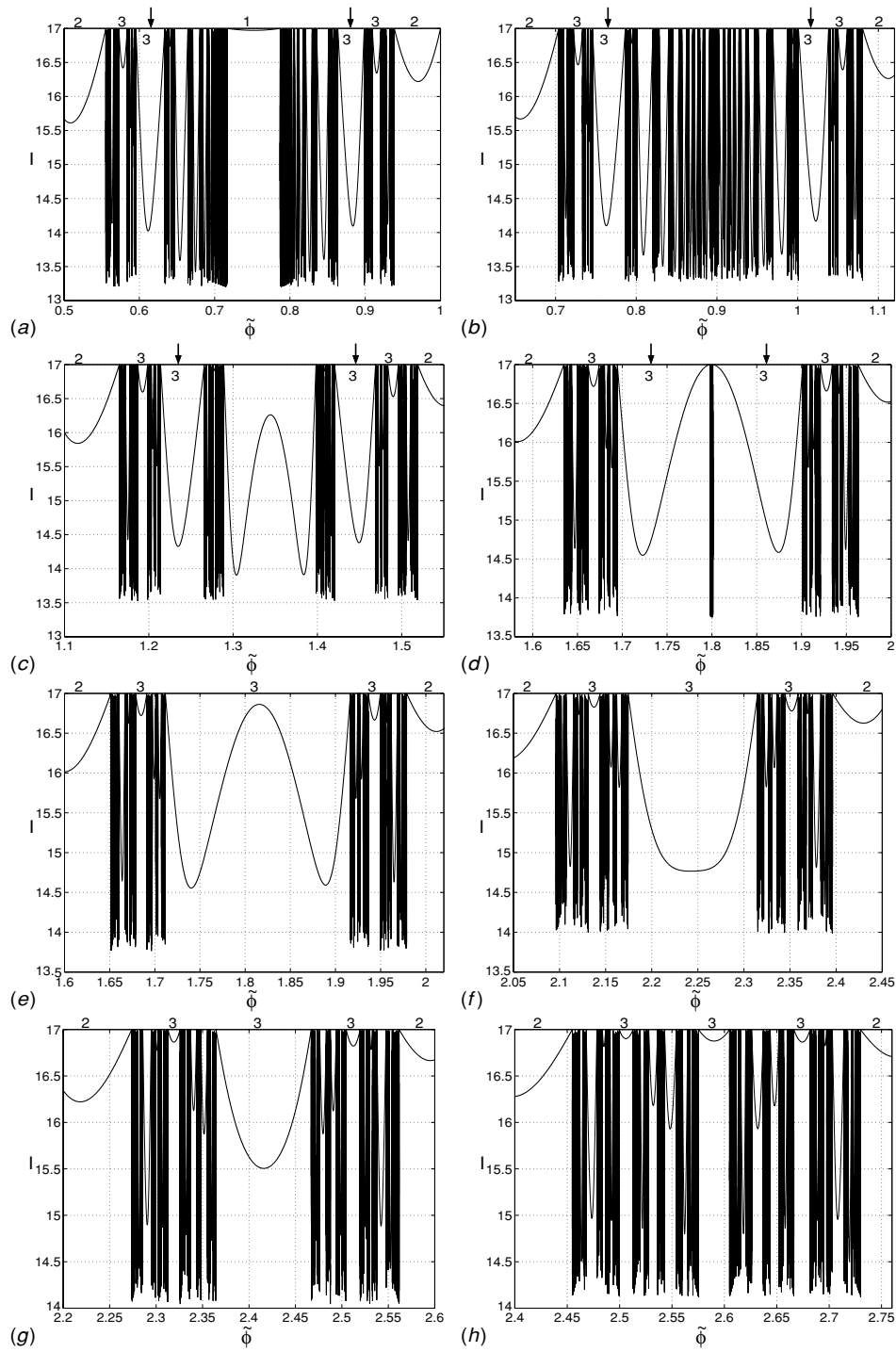


Figure 6. Sequence of plots of I versus $\tilde{\phi}$. In parts (a)–(h) C is 31, 30.5, 29, 27.55, 27.5, 26.2, 25.7, 25.2, respectively. $E = 17$ in all cases. Note the fusion and collision of extremal points and the change of extrema belonging to $\beta = 8/9$. The arrows on top of figures 6(a)–(d) mark the intervals $17/27$ and $19/27$.

pattern; how the tendrils of the stable manifolds belonging to the various levels of hierarchy intersect the local branch of the unstable manifolds. The hierarchical structure of this fractal can be cast into the form of a corresponding branching tree. For any value of the development parameter β there is a particular branching tree which characterizes this development stage uniquely. This pattern coincides with the pattern of singularities and intervals of continuity in the scattering function. Each interval of continuity (with the only exception mentioned above and treated in more detail below) produces exactly one rainbow singularity in the cross section. If we could see directly to which interval each singularity of the cross section belongs, then we would know which intervals exist for a particular case and thereby reconstruct the value of the development parameter. Therefore, the central point of our approach to the inverse problem is the identification of the various singularities in the cross section and in particular the information about which contributions have already disappeared in comparison with the complete case.

At the moment we do not see any possibility to see directly, in the cross section of a given general case, to which interval any singularity belongs. Therefore, we adopt the following strategy: we assume that we are able to change parameters in the system and in particular to change parameters along some curve in the possibly multidimensional parameter space which connects the case we are interested in with a case well in the region of completeness of the horseshoe. As we shall see below, it is not too difficult to make the identification of the various singularities for such a complete case. Then we go along the curve in parameter space in small steps and observe which singularities collide, appear and disappear along the curve. At the end, we check which singularities have survived in the actual case under study and this allows the reconstruction of the development parameter. Thereby, the topological structure of the chaotic set is obtained.

In addition, we will be able to recover the important scaling factors based on the idea mentioned in the previous section. The plots of the scattering function shown in figures 4–6 suggest that the form of the scattering function is basically the same in all intervals of continuity again with the only exception of those intervals which are in the process of fusion. Then the strength of the corresponding rainbow singularity is proportional to the length of the interval. Conversely, by measuring the strength (area under the peak) of the various peaks we get the length of the corresponding intervals and these are exactly the input data we need for the thermodynamical formalism to extract the measures of chaos. We only have to separate the contribution of any particular singularity from the background formed by the tails of all other rainbows. If in our particular case of a ternary symmetric horseshoe, with outer fixed points at infinity and, hence, outer fixed points with eigenvalues 1, the development parameter β is sufficiently large ($>1/2$) then the inner fixed point is unstable (inverse hyperbolic) and its eigenvalue is the dominant scaling factor of the whole dynamics. Thus, by measuring the scaling from one level of hierarchy to the next one we should extract easily an approximation to this eigenvalue.

As an example of demonstration we shall show the procedure for the parameter values used in figures 2 and 5 corresponding to a horseshoe of development stage $\beta = 8/9$ of our system. It is the horseshoe already shown in figure 2 with corresponding scattering function plotted in figure 5. To begin, in figure 7(a) we show the cross section for the *complete* case (corresponding to the horseshoe shown in figure 1 and the scattering function shown in figure 4). For the parameter values used, I_{\max} is very close to the value 17 and there are no contributions with I smaller than 12.2, therefore we restrict the plot to this interval in I . We see one large rainbow singularity around $I = 12.2$ coming from the minimum around $\tilde{\phi} = 3.1$ of the large interval of continuity. This interval corresponds to direct scattering, i.e., to trajectories not entering R . Next in strength is the singularity around $I = 16.6$. It corresponds

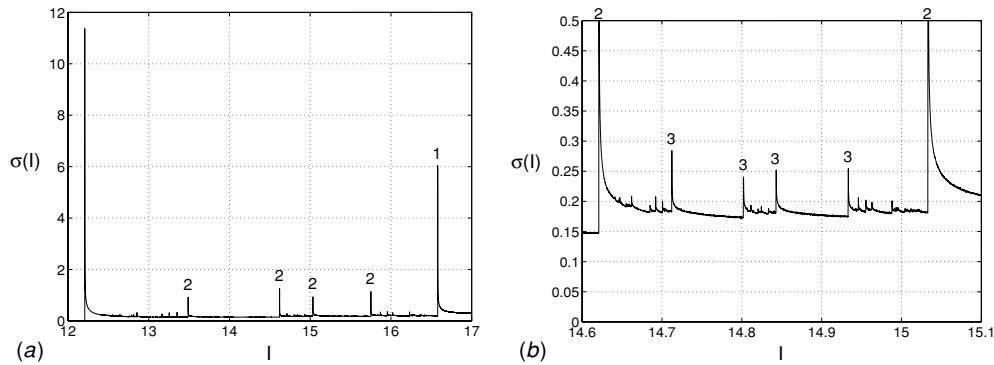


Figure 7. The cross section for the complete case. The parameters are the same as for figures 1 and 4. Part (a) shows the complete function $\sigma(I)$; part (b) is a magnification around one of the singularities of level 2, where the group of singularities of level 3 is identified.

to the only existing interval of hierarchical level 1. Next in strength come four singularities around $I = 13.5, 14.6, 15$ and 15.7 . They correspond to the four existing intervals of level 2. In the magnification, figure 4(b), we see weaker singularities of higher levels of hierarchy. It is easy to identify the group of singularities of level 3. The ratio of the strength of these singularities compared to any singularity of level 2 is approximately the same as the ratio of strengths of the level 2 compared to level 1. The numerical values of the ratios lie between 8 and 12, i.e., they lie around the value 10 of the eigenvalue of the inner fixed point.

Most important: in the complete case it is easy to identify the hierarchical level of all singularities of the first few levels only by seeing their strength in the cross section. It will not be necessary to know which rainbow belongs to which interval of the scattering function. To know the hierarchical level is sufficient. Let us assume we have identified all 12 singularities of level 3. As mentioned before in section 3, in this complete case there are $4 \times 3^{(n-2)}$ intervals of continuity of level n in the scattering function and thereby there is the same number of rainbow singularities in the cross section for hierarchical level n . Moreover, the scaling factor from any level to the next one is always approximately the same. Thereby in this complete case, we are able to identify the hierarchy number of all singularities up to a certain resolution, i.e., up to a certain level.

Now let us move along the parameter curve towards less developed horseshoes. How can we recognize when we have reached the development stage $\beta = 8/9$? From a plot of the corresponding horseshoe (remember figure 2 and its discussion) we see that this development stage is uniquely characterized by the following properties compared to the complete case: the interval of continuity of level 1 is already completely gone, all 4 intervals of level 2 are still present, from the 12 intervals of level 3 one is already completely gone and two other ones (the ones closest on either side to the middle interval of level 1) are fused. The contribution of level 1 disappears as soon as the horseshoe becomes incomplete. Then no further changes happen up to and including level 3 until we reach the development stage $\beta = 8/9$. We will study the events in $\beta = 8/9$ in all detail in the rest of this section.

As we approach the stage $\beta = 8/9$ from higher developments one interval of level 3 (it is the gap $25/27$ in the terminology of [5]) shrinks and its minimal value of I approaches the maximal allowed value of I . The corresponding singularity in the cross section moves to the upper allowed value of I while its total strength becomes weaker according to the shrinking length of the interval and exactly at the beginning of $\beta = 8/9$ it disappears completely. At the same time the complicated structure in between two intervals of continuity

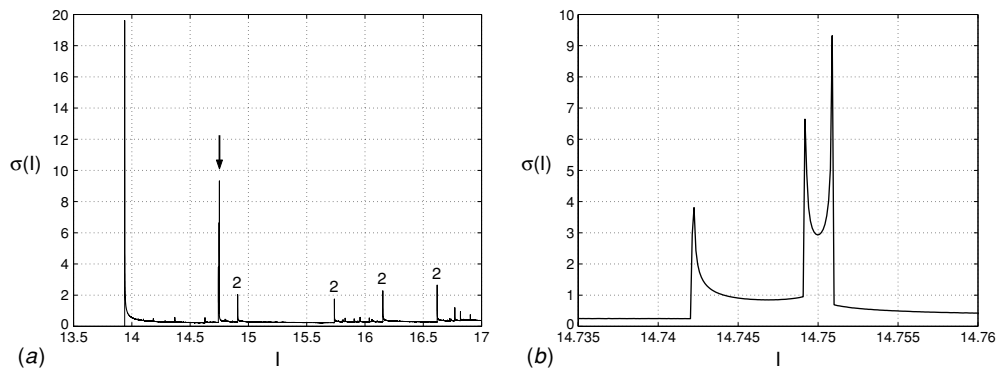


Figure 8. (a) The cross section for parameter values very close to the collision of the rainbows in the development stage $\beta = 8/9$. (b) A magnification of the degenerate peak, marked by an arrow in part (a). $E = 17$ and $C = 26.3$ as in figures 2 and 5.

of level 3 in the scattering function (the intervals $17/27$ and $19/27$, marked by arrows in figures 6(a)–(d)) shrink to nothing while the two intervals of level 3 fuse (cf, figure 6 and its discussion in the previous section). Also, this happens exactly when the development stage $\beta = 8/9$ begins. At the same time in this fused interval of level 3, a maximum of the function $I(\tilde{\phi})$ appears in the fusion point and it leads to a new singularity in the cross section. It has the opposite orientation compared to all the other singularities caused by minima of the scattering function; hence, it is easy to recognize. The two singularities corresponding to the minima of the two fused intervals continue without qualitative change at this point.

With a further change of the parameter, still within the development stage $\beta = 8/9$, the new maximum moves to smaller values of I and eventually collides with the two minima as shown in figure 6. In figure 8, we show a plot of the cross section very close to the collision point. Observe two features: first, the peak corresponding to the fused interval consists of a superposition of three rainbows, two with normal orientation and one with inverse orientation. In the plot it looks already similar to a single degenerate peak. Second, the total strength has grown sufficiently so that it is much stronger than the other peaks of level 3 and even than the peaks of level 2.

During the collision the three extremal points of the scattering function are turned into a single generic minimum. It produces a generic rainbow singularity in the cross section. Under a further parameter change the fused interval of level 3 shrinks, its minimal value of I increases, and finally approaches I_{\max} . At this point, the fused interval disappears and the development stage $\beta = 8/9$ ends. This scenario is presented graphically in figure 9 where we plot the position of all involved singularities of the cross section in the parameter/ I plane.

We summarize here this main result: the whole interval of parameter values which belongs to the development stage $\beta = 8/9$ is characterized uniquely as follows: it contains the first (when coming from the side of complete horseshoes) collision of singularities of level 3 in its interior. One of the singularities involved in this collision begins at the upper end of this parameter interval. The last one ends at the lower end of this parameter interval. Consequently, we can determine the limits of the region in parameter space where the development stage $\beta = 8/9$ is realized.

It is clear that we can identify parameter ranges belonging to other values of the development parameter β by observing collisions, appearance and disappearance of other singularities. Which ones belong to which development stage becomes clear from the study of schematic plots of horseshoes of the various development stages.

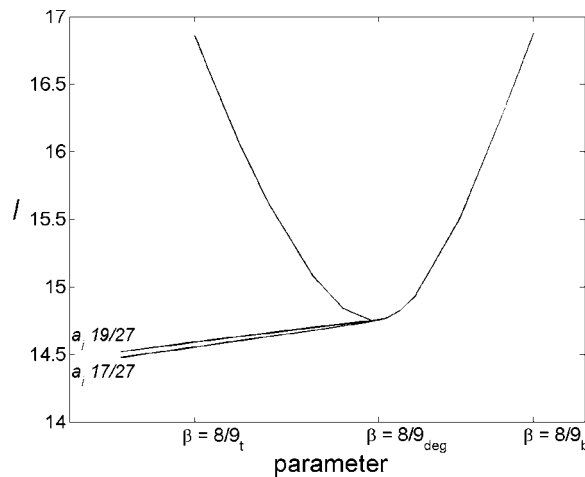


Figure 9. In the parameter/ I plane we show the position of the singularities belonging to the intervals $17/27$ and $19/27$ and their fusion and collision, appearance and disappearance. Curves a_i are the trajectories in parameter/ I space of rainbows $17/27$ and $19/27$. The parameter is C , varied from 28 to 25.2 with $E = 17$. $\beta = 8/9_t$ ($8/9_b$) is the top (bottom) limit of the development stage $\beta = 8/9$.

For an estimation of the scaling factors we should not include the fusing intervals and its corresponding singularities because of their degenerate nature. For the other contributions, we get an average value of $8.17\dots$ for the scaling from level 2 to level 3. This value is extremely close to the eigenvalue $8.18\dots$ of the inner fixed point.

6. Remarks and conclusions

We have demonstrated a new procedure for the classical inverse chaotic scattering problem. At the moment, we restrict ourselves to systems with one open and one closed degree of freedom because here any interval of continuity (with one possible exception) only produces a single singularity in the cross section. In many systems with two open degrees of freedom any interval produces an infinite sequence of singularities. To apply the same procedure to such systems it would be necessary to select one single singularity belonging to each interval (but it must be an equivalent one from each interval) and use it for the reconstruction. Interestingly, for the system treated in [14] (the scattering off three soft potential mountains in a two-dimensional position space), a pair of singularities from each interval can be selected easily as qualitatively different from the rest of the infinite sequence. Therefore, the method shown in the present paper could be applied to this system.

Now we come to the question of the generality of our procedure. The essential argument is based on *the structural stability* of the horseshoe development scenario which we must explain in some detail because of its importance for the relevance of the method. First, hyperbolic horseshoes are structurally stable [17]⁵. For our particular system, we have hyperbolicity only for the complete case. Therefore, if we start from a situation with a complete horseshoe and apply a sufficiently small perturbation to the Hamiltonian then the perturbed system also has a complete horseshoe with the same topological structure of intersections between stable and unstable manifolds of all periodic points. In this sense, the starting point

⁵ See especially pp 162–165, where it is explained why complete horseshoes fulfil axiom A and the transversality condition, which implies structural stability.

for our journey along a curve in parameter space remains unchanged. Second, we have to consider the stability of the development scenario as shown in figure 3. The essential steps on the development staircase are defined by the way in which the tips of the first level stable inner gaps end inside of some higher order unstable gaps. But such gaps have nonzero width. Therefore, this intersection property is structurally stable under small deformations of the horseshoe and thereby under small deformations of the system. Also, the deformed system has a development staircase of the same qualitative type; only the boundaries of the steps in the parameter space are continuously deformed. Most important, *the sequence and order of the important steps remain the same*. Consequently, we observe the same sequence of collision events of rainbow singularities under perturbations.

Our model here has two different discrete symmetries. What happens if the perturbations lift these symmetries? We begin by considering the reflection symmetry in y -direction. Without this symmetry we cannot use the reduced Poincare map. Then we have to choose one orientation of the intersection condition $y = 0$ and use only this one orientation. Accordingly, the Poincare map without this symmetry becomes the second iterate of the reduced Poincare map used in the symmetric system. Fortunately, the plot of the homoclinic tangle under any iterate of the map looks exactly the same; only the numbering of the hierarchical levels may become different. The fundamental point is that the topology of the intersection pattern between stable and unstable manifolds of the fixed points at infinity remains exactly the same. Therefore, also all conclusions drawn from this intersection pattern remain unchanged. Now we consider the reflection symmetry in the x -direction. Under a destruction of this symmetry the horseshoe in general turns into an asymmetric ternary one. Then we need two different development parameters, a β_{right} and a β_{left} which indicate to which degree the first-order inner tendrils of the manifolds coming from the right and the left outer fixed point penetrate into the fundamental rectangle. In the complete case, the horseshoe has the same qualitative structure and in particular the same topology as in the symmetric case. Only the scaling factors (and therefore also the rainbow singularity strengths) seen from the right and from the left are different in general. Even without symmetry in the parameter space we can identify steps on the development staircase where certain combinations of the two development parameters are realized (for a detailed discussion of a scattering system with an asymmetric ternary horseshoe with development parameters $\beta_{\text{left}} = 1$ and $\beta_{\text{right}} = 1/3$ and for its implications for the scattering behaviour see [18]). In the parameter space we connect these steps along some path in parameter space with the complete case and again study the change of the rainbow singularity structure along this path. In the nonsymmetric case, we have to study the cross section into the right-hand side channel and into the left-hand side channel simultaneously and the collision events in both channels are different.

If the obstacle potential, equation (2), were replaced by one with barriers, and accordingly with points of no return, then the outer fixed points would move to finite distance and become normal hyperbolic. This would avoid some technical difficulties encountered in the present physical model and in addition it would open the possibility for incomplete hyperbolic cases. They will even lead to structurally stable situations on some staircases of the development scenario.

In our case, the asymptotic potential in the y -direction is harmonic. Therefore, the return time in the Poincare map becomes independent of the action and therefore independent of the initial point as long as we are in the asymptotic region. Thereby, our case is very close to a system with one-dimensional position space and periodic time dependence where the stroboscopic map takes over the role of the Poincare map. For anharmonic oscillations in y -direction the return time in the Poincare map depends on the action. But this variable return time does not have any consequences for the topological structure of the horseshoe

nor for its development scenario. Consequently, no change is needed in our strategy for the reconstruction of horseshoe properties from cross section data.

Systems of the same qualitative structure as the one treated in detail in this paper can also be realized outside the domain of mesoscopic systems. An example is the collinear scattering of a particle from a bound state of two particles. Specifically, consider the nonreactive inelastic collinear collision of an isolated atom with a diatomic molecule, a process whose investigation has been reported frequently in the literature on chemical physics. The molecule has a single vibrational degree of freedom which for low excitation behaves like a harmonic oscillator, for higher excitation it becomes an anharmonic oscillator. For energies below the dissociation limit of the molecule, the vibrational degree of freedom is closed and we are exactly in the situation covered by the present paper.

We wish to point out that the basic strategy developed here does not depend on having a *ternary* horseshoe. For a system with a one-sided exit channel and a binary horseshoe the same basic idea can be applied to follow the development scenario of the binary horseshoe by observation of the collisions of rainbow singularities.

In total, all these considerations show that our method applies to a rather wide class of systems, namely, to scattering systems with one open and one closed degree of freedom. It includes systems with a one-dimensional position space and periodic time dependence. On the other hand, it is really essential to have only one open degree of freedom in order to have scattering functions with only one extremal point in non-degenerate intervals of continuity and as consequence with only a single rainbow singularity coming from each non-degenerate interval. Systems with two open degrees of freedom in general produce infinite sequences of rainbows coming from each individual interval. Thus, they fall outside the class of system which can be handled in analogy to our system of demonstration.

An important generalization to make in the future is to consider systems with more degrees of freedom. Then the first important task is to acquire a good understanding of higher dimensional horseshoe development scenarios. On this problem little is known at the moment.

We emphasize that the important advantage of the present approach, over all the methods presented in [5–8] for the inverse chaotic scattering problem, is that we only need *cross sections as input data*, i.e., the information which is usually measured in scattering experiments. The knowledge of scattering functions is not needed. Therefore, it makes sense to try to generalize the idea to quantum dynamics and to evaluate the pattern of the corresponding wave dynamical rainbows.

One part of the strategy of the present work, namely, to follow the system in parameter space from a known case (here the complete one) to the unresolved case we are actually interested in, could also be applied to the following problem: if we have the *scattering* functions and want to use them to reconstruct the horseshoe, then the greatest problem is the identification of the hierarchical level of the various intervals of continuity. So far in [5] and [7] this problem has only been solved for systems with one open and one closed degree of freedom. For more complicated systems with two degrees of freedom we could start from a known case, in particular the complete case where we have identified all intervals of continuity, and study the change of the structure of intervals and singularities in the scattering function along a curve in parameter space. By observing which intervals fuse and disappear we can determine the development stage we actually have.

Acknowledgments

The authors are grateful to CONACyT, Mexico and VIEP-Conacyt for partial support of this project. GAL-A thanks the Mercator-Professorship Programme, Germany.

References

- [1] Ramm A G 1992 *Multidimensional Inverse Scattering Problems* (New York: Longman Scientific/Wiley)
- [2] Gladwell G M L 1993 *Inverse Problem in Scattering. An Introduction* (Dordrecht: Kluwer)
- [3] Akharies B N and Sucko A A 1990 *Potential and Quantum Scattering. Direct and Inverse Problems* (Berlin: Springer)
- [4] 1993 CHAOS **3** (whole issue)
- [5] Jung C, Lipp C and Seligman T H 1999 *Ann. Phys.* **275** 151
- [6] Bütikofer T, Jung C and Seligman T H 2000 *Phys. Lett. A* **265** 76
- [7] Tapia H and Jung C 2003 *Phys. Lett. A* **313** 198
- [8] Jung C, Merlo O and Seligman T H 2005 CHAOS **14** 969
- [9] Tel T 1990 *Directions of Chaos* vol 3 ed B L Hao (Singapore: World Scientific) p 149
- [10] Luna-Acosta G A, Orellana-Rivademyra G and Jung C in preparation
- [11] See, e.g., Datta S 1995 *Electronic Transport in Mesoscopic Systems* (Cambridge: Cambridge University Press)
- [12] See, e.g., Granot E 2000 *Phys. Rev. B* **61** 11078
Tekman E and Ciraci S 1990 *Phys. Rev. B* **42** 9098
Boese D, Lischka M and Reichl L E 2000 *Phys. Rev. B* **62** 16933
Singha Deo P, Bandopadhyey S and Das S 2002 *Int. J. Mod. Phys. B* **16** 2247
- [13] Davies M J, MacKay R S and Sannami A 1991 *Physica D* **52** 171
- [14] Jung C and Pott S 1989 *J. Phys. A: Math. Gen.* **22** 2925
- [15] Jung C 1991 *The Electron: New Theory and Experiment* ed D Hestenes and A Weingartshofer (Dordrecht: Kluwer)
- [16] Newton R G 1982 *Scattering Theory of Waves and Particles* 2nd edn (New York: Springer)
- [17] Palis J and de Melo W 1982 *Geometric Theory of Dynamical Systems* (New York: Springer)
- [18] Emmanouilidou A, Jung C and Reichl L E 2003 *Phys. Rev. E* **68** 046207